DOI: 10.5137/1019-5149.JTN.12681-14.0
Received: 14.10.2014 / Accepted: 08.01.2015
Published Online: 16.02.2016

Original Investigation

Construction of Finite Element Model for an Artificial Atlanto-Odontoid Joint Replacement and Analysis of Its Biomechanical Properties

Yong HU[1], Wei-xin DONG[1], Shannon HANN[2], Zhen-shan YUAN[1], Xiao-yang SUN[1], Hui XIE[1], Meichao ZHANG[3]

[1]The Affiliated Ningbo No.6 Hospital of Medical School of Ningbo University, Department of Spinal Surgery, Ningbo, Zhejiang Province, China
[2]Thomas Jefferson University & Rothman Institute, Department of Orthopaedic Surgery, Philadelphia, Pennsylvania, USA
[3]Southern Medical University, Department of Medical Biomechanics Research, Guangzhou, Guangzhou Province, China

ABSTRACT

AIM: To investigate the stress distribution on artificial atlantoaxial-odontoid joint (AAOJ) components during flexion, extension, lateral bending and rotation of AAOJ model constructed with the finite element (FE) method.

MATERIAL and METHODS: Human cadaver specimens of normal AAOJ were CT scanned with 1 mm -thickness and transferred into Mimics software to reconstruct the three-dimensional models of AAOJ. These data were imported into Freeform software to place a AAOJ into a atlantoaxial model. With Ansys software, a geometric model of AAOJ was built. Perpendicular downward pressure of 40 N was applied to simulate gravity of a skull, then 1.53 N• m torque was exerted separately to simulate the range of motion of the model.

RESULTS: An FE model of atlantoaxial joint after AAOJ replacement was constructed with a total of 103 053 units and 26 324 nodes. In flexion, extension, right lateral bending and right rotation, the AAOJ displacement was 1.109 mm, 3.31 mm, 0.528 mm, and 9.678 mm, respectively, and the range of motion was 1.6°, 5.1°, 4.6° and 22°.

CONCLUSION: During all ROM, stress distribution of atlas-axis changed after AAOJ replacement indicating that AAOJ can offload stress. The stress distribution in the AAOJ can be successfully analyzed with the FE method.

KEYWORDS: Biomechanics, Finite element method, Atlanto-odontoid joint, Atlanto-axial joint, Arthroplasty

■ INTRODUCTION

The anterior high cervical spine fusion technique is often performed to relieve ventral compression and to improve the stability of the craniovertebral junction (CVJ) (8,10,17,24). Some of the indications include congenital atlanto-occipital fusion induced C1-C2 joint laxity and chronic dislocation; basilar invagination; congenital odontoid malformation caused C1-C2 dislocation; rheumatoid arthritis induced compression and C1-C2 dislocation; and brainstem and cord compression from CVJ tumors. These are typically treated by transoral decompression combined with posterior fusion (1,2,5). However, intraoperative flipping of a patient may aggravate cervical spinal cord injury. To solve this problem, some (1,28) have adopted the transoropharyngeal atlantoaxial reduction plate (TARP); however, this fusion technique restricts normal physiological range of motion (ROM) of the upper cervical spine. Several prospective studies of artificial atlanto-odontoid joint (AAOJ) replacement have been reported (11-13,18) but finite element biomechanical analysis of AAOJ has not yet been reported to the authors knowledge. We reported a design of an AAOJ that can not only rebuild the stability of the atlanto-axial joint, but also reserve the rotation function

Corresponding author: Yong HU
E-mail: huyong610@163.com

between atlas and axis. This AAOJ is suitable for restoring physiological function of C1-2 after surgical decompression of CVJ (11). However, like other artificial joints, AAOJ also has problems of prosthesis loosening, wearing, etc. This paper constructed a FE model of atlantoaxial joint after AAOJ replacement, analyzed the stress distribution, determined the range of motion (ROM), and evaluated the biomechanical stability of the joint, so as to validate its efficacy and to provide a theoretical basis for AAOJ development and clinical application.

■ MATERIAL and METHODS

Main components and properties of AAOJ

The designed AAOJ is divided into atlas and axis components. The atlas component is composed of atlas rotating sleeve and lateral mass fixing plate, while the axis component includes axial rotation axis, axial base and lateral mass fixing plate. AAOJ is made of titanium alloy Ti-6Al-4V whose mechanical strength, corrosion resistance and anti-fatigue properties are superior to stainless steel or cobalt chromium alloy but with poor wear resistance.

Atlanto-axial joint geometric model after AAOJ replacement

A fresh cervical cadaveric specimen (male, 28 years old, height: 174 cm, weight: 70 kg) was selected, and the open mouth view of upper cervical spine and cervical lateral X-rays were obtained to exclude cervical disease. The atlas and axis were cleared of the ligaments, muscles and other soft tissues. Both Occiput to C2 and AAOJ were imaged with volumetric computed tomography (CT) scanning (Philips Brilliance 64 CT, Philips Medical Systems, Netherland) with 1-mm slice thickness and then stored in Digital Imaging and Communications in Medicine (DICOM) format to create 3D models of the atlas-axis complex and AAOJ. Both models were transferred in STL (Stereo Lithography) format to the Freeform Software (U.S. Phantom) and then, with reference to clinical practice, the anterior arch of the atlas, dens and part of the axis were removed to simulate anterior decompression. The artificial atlanto-axial joint model was installed into the decompressed atlanto-axial model. During the installation, the relation between the atlas/axis and screws were defined as union, which simulates fixation in a non-loosening state; the relation of the locking screws and plate was defined as being locked, and the artificial atlanto-axial joint was defined as contact. Using the pavement function of Freeform software, all components of the integrated artificial atlanto-axial joint model were imported to Ansys software in IGES format to build an artificial atlanto-axial joint geometric solid model (Figure 1A,B). The material properties of each component and the unit node information are demonstrated in Table I.

Constructing mesh model, ligaments and joint contact

Using the Ansys self-adaptive meshing design, the model was meshed with the solid185 tetrahedral element solid model

Table I: Material Properties Used in the Finite Element Model

Components	Young's Modulus (MPa)	Poisson's Ratio	Units	Node
Cancellous bone	500	0.25	23187	5744
Cortical bone	10000	0.25	17613	6012
Titanium alloy	11300	0.25	61547	14005
Articular ligaments	7	0.25	159	318
Interspinal ligaments	8		14	28
Supraspinal ligaments	8		8	16
Cartilage	20	0.25	525	201
Contact elements			4388	2296

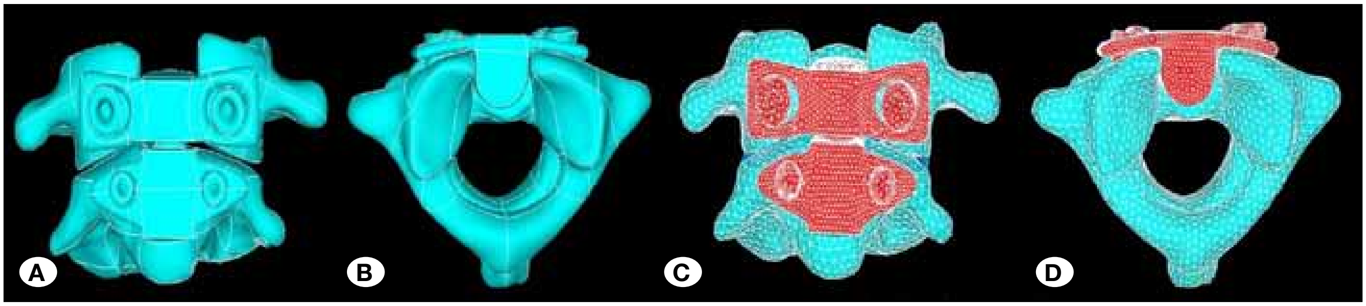

Figure 1: The C1-2 constructed with AAOJ. **A)** Geometric model in anterior view, **B)** Geometric model in superior view, **C)** Mesh model in anterior view, **D)** Mesh model in superior view.

with careful control of the mesh density. The related ligament structures in the model were added to the mesh model. The involved ligaments were as follows: atlanto-axial ligaments, zygapophysial joint capsular ligament, interspinous ligament, supraspinous ligament. The solid model (atlanto-axial cortical bone, cancellous bone and AAOJ) was assumed as the solid185 tetrahedral element, and the ligament was defined as a low elastic two-node cord unit, which cannot transfer the stress. Each ligament was defined with different elastic modulus according to the neutral zone and elastic zone (22) to simulate the non-linear property of ligaments. Sliding contact definition with a friction coefficient of 0.1 was used for the facet joints between the bilateral atlanto-axial joints and AAOJ (4). The relationship between vertebrae and screws, screws and plate, and atlas plate and axis plate were defined as closely binding, non-loosening contact, and frictionless contact respectively. Figure 1 C,D show the final mesh model.

Border constraint, load setting, and validation of the three-dimensional FE model after AAOJ replacement

The displacement in each direction at all the nodes along the lower edge of C2 was set as 0 mm. A fixed handle above the atlas was designed to simulate the occipital bone. A 40 N perpendicular downward pressure on the fixed handle was applied to simulate the gravity of skull, then 1.53 N • m torque was exerted separately to simulate flexion, extension, lateral bending and rotation while observing the stress distribution of AAOJ components in each motion. Each unit had adequate stability under stress, and force deformation of materials and the micromotion between the screws and bone were not taken into account. With the lower plane of axis as a fixed point, the stress on the atlantoaxial joint in flexion, lateral bending, extension, rotation after AAOJ replacement were recorded. The analysis included two parts: 1. Contrast validation was performed with our previous biomechanical results (13) and if the angular displacements under the same load were similar, the model was regarded as valid; 2. Self-validation.

Table II: The Comparison Between the FE Model of C1-C2 and Biomechanical Experiment in Vitro (Hu et al. (13))

Item	Hu et al (13) $C_{1\sim2}$	FE model $C_{1\sim2}$
Bending moment (Nm)	1.5	1.5
Flexion (°)	5.5±0.9	1.6
Extension (°)	4.8±0.9	5.1
Lateral bending (°)	1.4±0.4	4.6
Rotation (°)	32.7±3.8	22

RESULTS

Atlanto-axial joint geometric model validation after AAOJ replacement

The three-dimensional model of the artificial atlanto-axial joint before and after assembly (Figure 2A-F), the geometric solid model of the atlanto-axial joint (Figure 1 A,B) after AAOJ replacement, and the FE model after ligament loading and meshing (Figure 1 C,D) showed an excellent bionic effect and geometric similarity. A total of 103,053 units and 26,324 nodes comprised this model. After loading on the FE model, the stress and displacement data for all nodes were obtained. The displacement of AAOJ was 1.109 mm, 3.31 mm, and 0.528 mm in flexion, extension, and right lateral bending respectively, which was relatively small. The displacement in right rotation was 9.678 mm. After further calculation and analysis, the ROM of the artificial atlanto-axial joint in each position was determined and these are illustrated in Table II (Figure 5). It was proved that the angular displacement of each functional unit of the model was inline with our previous in vitro biomechanical experimental results (13) (Table II), in which the

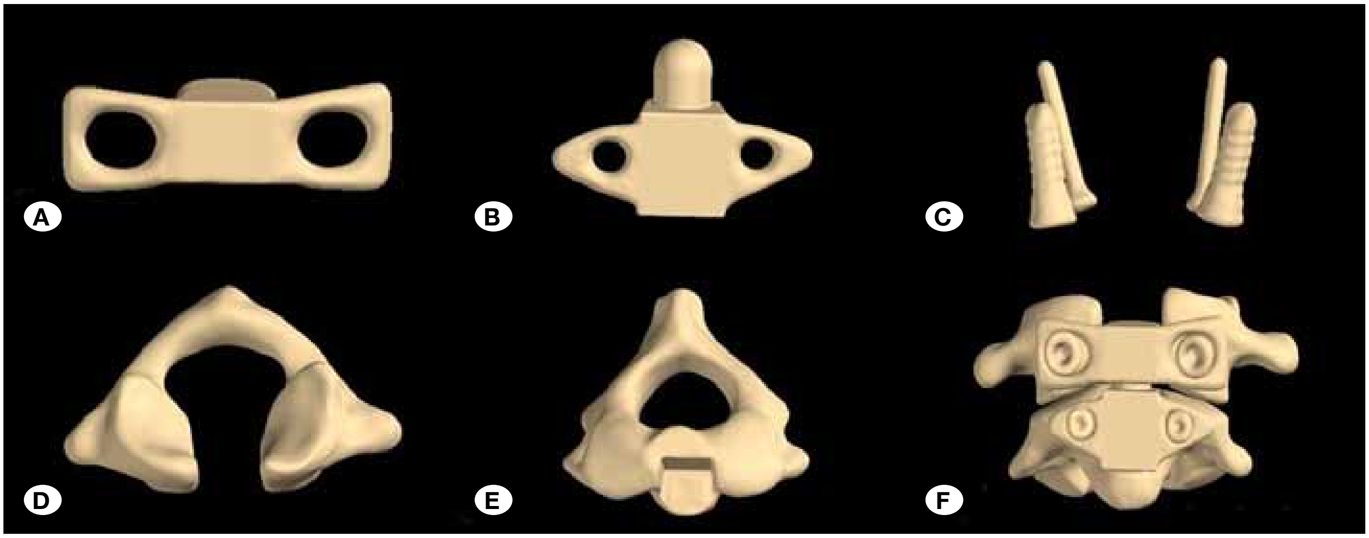

Figure 2: The 3-D model. **A)** Atlas part of AAOJ, **B)** Axis part of AAOJ, **C)** Screws, **D)** C1 without anterior arch, **E)** Dredged part of vertebral bone at C2 , **F)** The C1-2 constructed with AAOJ.

values in rotation and lateral bending were unilateral. The FE model of the atlanto-axial joint after AAOJ replacement was based on CT scan data of human atlanto-axial specimens and their corresponding artificial joint, and refined by Freeform software and thus showing high shape accuracy.

FE analysis on biomechanical properties of the atlanto-axial joint bone structure after AAOJ replacement

In anterior flexion, besides the screw holes, the stress was mainly concentrated at the junction of atlas lateral mass and atlas posterior arch, which were also the affected area of typical Jefferson fracture, with the maximum stress value of 0.138×10^8 N / m^2. The stress at axis was mainly concentrated at screw holes, the contact surface of the plate and axis, and axial vertebral arch, with the maximum stress value of 0.201 $\times 10^8$ N / m^2 (Figure 3A,B). In extension, the stress of atlas is mainly concentrated at the junction of lateral mass and pedicle, with the maximum stress value of 0.666×10^7 N / m^2; and the stress of axis was mainly concentrated in contact area of axis and plate. The vertebral arch also presented obvious stress concentration, with the maximum stress value of 0.254 $\times 10^8$ N / m^2; and stress concentration also existed at the screw holes of both atlas and axis (Figure 3D,E). In right lateral bending, the stress of atlas focused on the screw hole of right lateral mass, with a maximum stress value of 0.124×10^8 N / m^2; besides axial vertebral arch, the contact site of axis and right side of plate bore the maximum stress concentration, with the maximum stress value of 0.178×10^8 N / m^2 (Figure 3 G,H). In right rotation, besides screw holes, the border of bilateral atlas posterior arch and lateral mass endured the maximum stress concentration, with a maximum stress value of 0.847×10^7 N / m^2. As for axial stress distribution, besides the screw holes, the maximum stress concentration was at the contact of axis with the plate, with a maximum stress value of 0.170×10^9 N / m^2 (Figure 3 J,K).

FE analysis on the biomechanical properties of AAOJ components after AAOJ replacement

In flexion, the stress distribution of each component is illustrated in Figure 3C. The maximum stress value of the atlas plate was 0.292×10^8 N / m^2, and the stress was mainly focused on screw holes and the contact area with the artificial dens; the maximum stress value at axis plate was 0.911×10^8 N / m^2, the stress was mainly focused on screw holes and the contact part of plate and axis.

In extension, the stress distribution of components is illustrated in Figure 3F. The maximum stress value of atlas plate was 0.287×10^9 N / m^2 and the stress was mainly focused on screw holes and the contact with the artificial dens. The maximum stress value at axis plate was 0.396×10^9 N / m^2 which was mainly focused on screw holes and above the spacing hole anterior to the plate.

In right lateral bending, the stress distribution of components is illustrated in Figure 3 I. The maximum stress value of the atlas plate was 0.176×10^9 N / m^2 and the stress was mainly focused on screw holes and the contact with the artificial dens (above the left lateral wall of dens hole). The maximum stress value at axis plate was 0.345×10^9 N / m^2 which was mainly focused on screw holes and above the left lateral wall of artificial dens.

In right rotation, the stress distribution of components is illustrated in Figure 3L. The maximum stress value of the atlas plate was 0.133×10^9 N / m^2 and the maximum stress concentration was at screw holes and locking holes The maximum stress value at axis plate was 0.124×10^9 N / m^2 which was mainly focused on screw holes and locking hole.

In flexion and extension, high stress was present at the root of axial screws, but not at the atlas screw root, as shown in Figure 3C,F. The maximum stress value was 0.345×10^9 N / m^2 in the anterior flexion, 0.403×10^9 N / m^2 in the posterior extension.

FE analysis on three-dimensional stability of the atlanto-axial joint after AAOJ replacement

Three-dimensional displacement of the atlanto-axial joint in four working conditions under different loads is demonstrated in Figure 4A-H. The symmetrical data between left and right side showed no significant difference ($p > 0.05$). The displacement of AAOJ was 1.109 mm, 3.31 mm, 0.528 mm in flexion, extension, and right lateral bending respectively, which were relatively small. The displacement in right rotation is 9.678 mm. According to the overall displacement and the configuration of this model, using trigonometric function, ROM was 1.6°, 5.1°, 4.6° and 22° in flexion, extension, right lateral bending and right rotation respectively.

■ DISCUSSION

The first problem is to find a feasible model that is the basis of subsequent meshing and FE analysis. It determines the accuracy and speed of the FE calculation. We simplified the structure of the model based on the smallest functional segment, making it more convenient for the following bio-mechanical analysis. The established model shows good morphological similarity to the atlanto-axial joint after AAOJ replacement. Compared with the biomechanical analysis of specimens, FE analysis has some advantages. It can simulate the complex geometric structure of cervical vertebrae in computer based on the scan data (6,16,20,26), and the experiments can be repeated dozens of times in computers cutting the cost (7,21,29). The biomechanical experiments on specimens can only measure the mechanical properties of bone surface, while FE analysis show high efficiency on mechanical analysis of the internal structure of the cervical vertebrae. In addition, the traditional biomechanical analysis cannot well reflect the influence of the surrounding tissues on cervical spine but in FE analysis we can set some supplemental conditions, allowing it to achieve a bionic effect to a certain degree. Therefore the biomechanical results of FE model analysis can validate (15) a more comprehensive understanding of biomechanical changes in cervical joint activities. So far, there have been no reports on the FE analysis of AAOJ in literature domestically or abroad.

Under an axial static compressive load, stress on C1 cadaveric specimen and C1 Finite Element model is mainly

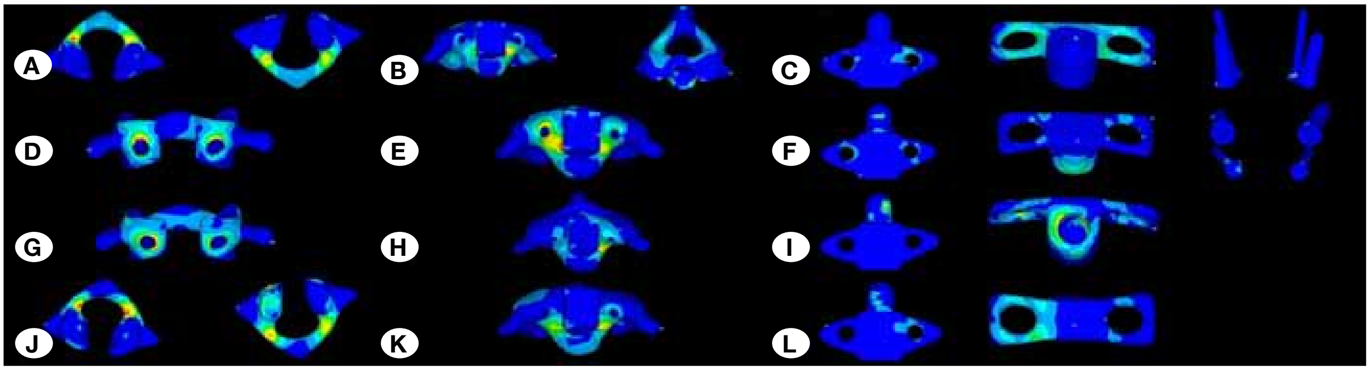

Figure 3: Stress distribution. **A)** C1 flexion in superior and inferior, **B)** C2 flexion in anterior and superior, **C)** AAOJ and screws in flexion, **D)** C1 extension, **E)** C2 extension, **F)** AAOJ and screws in extension, **G)** C1 right bending, **H)** C2 right bending, **I)** AAOJ in right bending **J)** C1 right rotation in superior and inferior, **K)** C2 right rotation, **L)** AAOJ in right rotation.

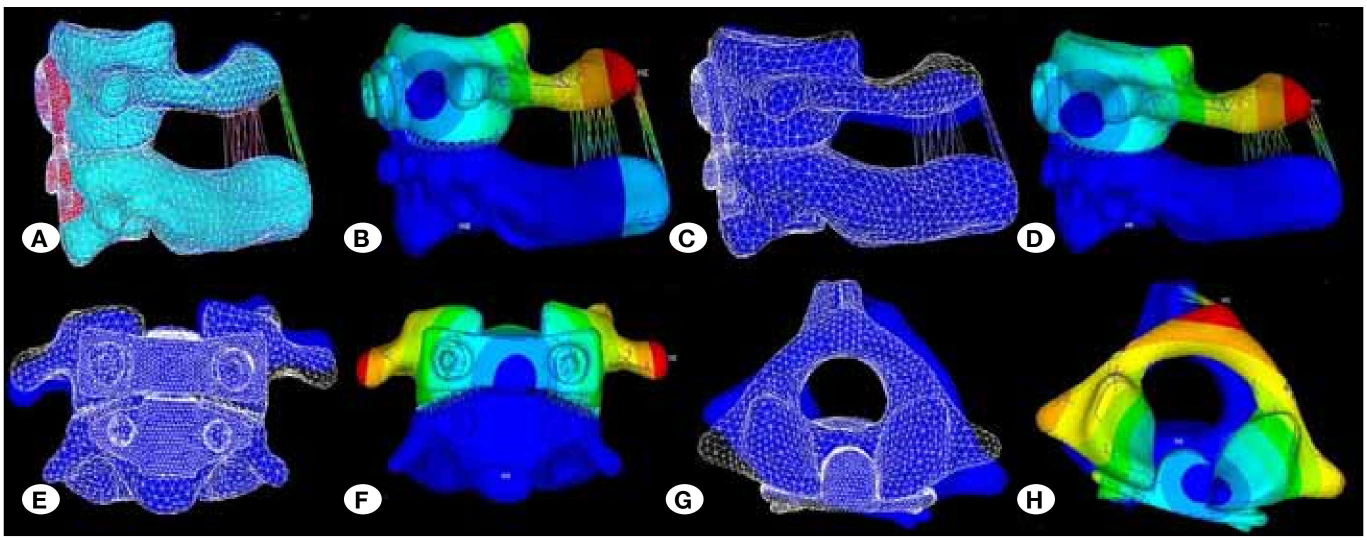

Figure 4: The displacement and its numerical value. The model combined by the white dotted line was at the original position, and the model combined by the blue was moving from the original position. **A,B)** Flexion, **C,D)** Extension **E,F)** Right bending, **G,H)** Right rotation.

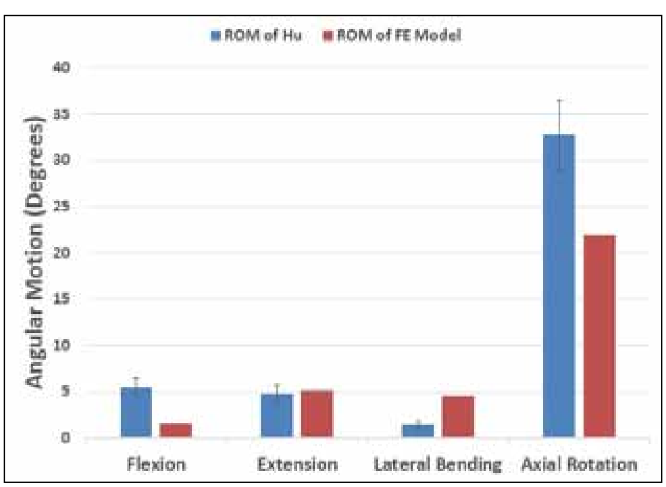

Figure 5: Comparisons of the ROM under pure moment of 1.5 Nm between biomechanical experiment in vitro studies (Hu et al. (13)) and the present study.

concentrated on the anterior arch and posterior arch (9). Our study demonstrated that after the AAOJ replacement, stress increased on the screw holes and the junction of lateral mass - posterior arch, the stress at a hole was gradually transferred to its periphery, while the stress at the junction of lateral mass - posterior arch passed to posterior arch. The stress concentration at the junction of atlas lateral mass - posterior arch is still a potential risk factor of fractures, such as a Jefferson fracture. The mechanism of a Jefferson fracture is related to the junction of lateral mass of atlas and anterior/posterior arch is the vulnerable spot, coupled with axial stress acts on the atlas (3). Atlas pedicle screw fixation may be performed to increase the load capacity; however, taking the risk of vertebral artery injury by screws into account (25), atlas was fixed with single cortical, hollow, lateral mass screws with lateral holes. As long as single cortical lateral mass screws of atlas do not penetrate the posterior surface of lateral mass, the fixation can be regarded as safe from the anatomical point of view (19). Atlas screw hole stress (take posterior extension for example) is mainly concentrated in the upper edge of the screw hole and distributed to lateral mass, because in extension, the atlas rotating sleeve is restricted by artificial dens, and the atlas component is not integrated with the atlas so resistant micromotions will lead to the loosening of the artificial joint. In this study, the atlas components of AAOJ were fixed by hollow screws with side holes to avoid the above mentioned problems. During implantation, bone particles can get into the hollow part through the lateral holes of the screws. Theoretically, the screws could achieve bone fusion with the atlas lateral mass *in vivo*, thus increasing the interface and improving the biomechanical properties of the atlas. This design overcomes the disadvantage that bone-screw connection is not strong enough, reducing the risk of prosthesis loosening, and increasing the overall stability of AAOJ fixation. Similar to the atlas, the stress of axis is mainly concentrated on the screw holes, pedicle and contact area of axial components and axis. However, in the long run, the axis component can combine with the bone structure better than atlas to achieve better stability because the base of axis component is wedge-shaped which makes it more accommodating (13). The axis component is fixed by bicortical pedicle screws to offer better stability of the axial components.

The results of this study showed that high stress was observed in the axis screw roots, but not in the atlas screw roots in flexion/extension. The maximum stress value was 0.345×10^9 N in flexion, 0.403×10^9 in extension. This may be due to the fact that the atlas screw has a longer diameter and larger contact surface with plate compared with the axis screw. This suggests that the axis screw is prone to breakage after replacement of AAOJ, making it important to augment the axis screw hardness, and to reduce the stress distribution on axis screws, which can be achieved by increasing the diameter of screw head, and coating the screw surface with polymer materials. Hussain et al. (14) made a FE analysis to study the influence of different screw angles on the stability of the model after anterior cervical vertebrectomy and plate internal fixation. The results showed that the appropriate angle of the screw can reduce the stress on bone graft, endplate, and the screws, thereby reducing the internal fixation failure. In the safety analysis on the screw trajectory of atlanto-axial components of AAOJ, the atlas screws had a certain range of extroversion angle, and the axis screws had a certain range of extroversion or posteroversion angles during the AAOJ replacement, making it better to determine the right angle of the screw to reduce the corresponding stress as much as possible.

In all ROMs, stress concentration is mainly on the plate holes and the contact sites of atlanto-axial components in AAOJ, especially the locking holes, and the contact sites of the axis plate with the bone. This can cause abrasion, prosthesis loosening, and even dislocation. The stress concentration may be attributed to the fact that the two parts of this device, the atlas and axis, are not integrated closely. Designing a connective structure of both can solve this problem. Scholes and Unsworth (23) thought that improving the lubrication between the articular surfaces is the most important means to reduce friction and wear in artificial joints.

The atlanto-axial joint is a rotary joint along central axis with relatively large mobility. In normal rotation of neck, the atlanto-odontoid joint revolves with a constantly changing center of rotation or multiple rotation centers, rather than along a fixed axis. This study showed that after AAOJ replacement, the ROM of atlanto-axial joint was 1.6°, 5.1°, 4.6° and 22° in flexion, extension, right lateral bending and right rotation, respectively. This is consistent with previous studies on cadaver, indicating that this modified AAOJ can not only stabilize the vertebrae but also retain the mobility. We analyzed the following conducive aspects: 1) Atlas rotating sleeve and axial rotation axis work closely together to rebuild the button-lock relationship of atlas odontoid joint, so that the axis of rotation is relocated to the atlas odontoid joints, thereby restricting flexion, extension and axial lateral bending. 2) Excessive sliding is restricted because the angular movement of the normal atlanto-axial joint should couple with sliding, and the limited sliding ROM actually confines the ROM of angular movement. ROM of normal atlas-axis in flexion-extension and lateral bending is limited and mainly accounted by the atlanto-occipital joint and cervical intervertebral joints below the axis (including the vertebral disc and the lateral mass joints) (27). After AAOJ replacement, the reduction of ROM of atlanto-axial joint in flexion, extension and lateral bending has little impact on the movement of head and neck (19). Lu et al. (19) designed a restriction structure in artificial joint to prevent over-rotation. The originality of our design lies in the locking holes, AAOJ can achieve the rotation of 22° under 1.53 N• m torque, which is not beyond the normal ROM.

■ CONCLUSION

During all ROM, stress distribution of atlas-axis changed after AAOJ replacement indicating AAOJ can offload stress. The stress distribution in the AAOJ can be successfully analyzed with the FE method.

■ REFERENCES

1. Ai FZ, Yin QS, Xu DC, Xia H, Wu ZH, Mai XH: Transoral atlantoaxial reduction plate internal fixation with transoral transpedicular or articular mass screw of C2 for the treatment of irreducible atlantoaxial dislocation: Two case reports. Spine 36: E556-562, 2011
2. Ashraf J, Crockard HA, Ransford AO, Stevens JM: Transoral decompression and posterior stabilisation in Morquio's disease. Arch Dis Child 66:1318-1321, 1991
3. Bozkus H, Karakas A, Hancı M, Uzan M, Bozdag E, Sarioglu AC: Finite element model of the Jefferson fracture: Comparison with a cadaver model. Eur Spine J 10: 257-263, 2001
4. Brolin K, Halldin P: Development of a finite element model of the upper cervical spine and a parameter study of ligament characteristics. Spine: 29: 376-385, 2004
5. Crockard HA, Pozo JJ, Ransford AO, Stevens JM, Kendall BE, Essigman WK: Transoral decompression and posterior fusion for rheumatoid atlanto-axial subluxation. J Bone Joint Surgery BR 68: 350-356, 1986

6. del Palomar AP, Calvo B, Doblaré M: An accurate finite element model of the cervical spine under quasi-static loading. J Biomech 41: 523-531, 2008
7. Dickinson AS, Taylor AC, Ozturk H, Browne M: Experimental validation of a finite element model of the proximal femur using digital image correlation and a composite bone model. J Biomech Eng 133: 014504, 2011
8. Dickman CA, Sonntag VK: Posterior C1-C2 transarticular screw fixation for atlantoaxial arthrodesis. Neurosurgery 43: 275-280, 1998
9. Gebauer M, Goetzen N, Barvencik F, Beil FT, Rupprecht M, Rueger JM, Puschel K, Morlock M, Amling M: Biomechanical analysis of atlas fractures: A study on 40 human atlas specimens. Spine 33: 766-770, 2008
10. Guo X, Ni B, Zhao W, Wang M, Zhou F, Li S, Ren Z: Biomechanical assessment of bilateral C1 laminar hook and C1-2 transarticular screws and bone graft for atlantoaxial instability. J Spinal Disord Tech 22: 578-585, 2009
11. Hu Y, Yang SH, Xie H, Xu RM, Ma WH: Quantitative anatomic study of atlanto-odontoid joint and design of an artificial atlanto. Odontoid joint for the orthopedic clinic. Chin J Traumatol 10: 138-144, 2007
12. Hu Y, Yang S, Xie H, He X, Xu R, Ma W, Feng J, Chen Q: The anatomic study on replacement of artificial atlanto-odontoid joint through transoral approach. J Huazhong Univ Sci Technology Med Sci 28: 327-332, 2008
13. Hu Y, Gu Yj, He Xf, Xu RM, Ma WH, Zhao WD, Liang DZ, Zhong SZ: Biomechanical evaluation of stability and three-dimensional movements of the atlantoaxial joint after artificial atlanto-odontoid joint arthroplasty. Orthop Surg 2:111-118, 2010
14. Hussain M, Nassr A, Natarajan RN, An HS, Andersson GB: Biomechanical effects of anterior, posterior, and combined anterior-posterior instrumentation techniques on the stability of a multilevel cervical corpectomy construct: A finite element model analysis. Spine J 11: 324-330, 2011
15. Hussain M, Natarajan RN, Chaudhary G, An HS, Andersson GB: Simulation of inhomogeneous rather than homogeneous poroelastic tissue material properties within disc annulus and nucleus better predicts cervical spine response: A C3–T1 finite element model analysis under compression and moment loadings. Spine 36: E245-255, 2011
16. Imajo Y, Hiiragi I, Kato Y, Taguchi T: Use of the finite element method to study the mechanism of spinal cord injury without radiological abnormality in the cervical spine. Spine 34:E83-87, 2009
17. Lapsiwala SB, Anderson PA, Oza A, Resnick DK: Biomechanical comparison of four C1 to C2 rigid fixative techniques: Anterior transarticular, posterior transarticular, C1 to C2 pedicle, and C1 to C2 intralaminar screws. Neurosurgery 58:516-521, 2006
18. Lu B, He XJ, Zhao CG, Li HP, Wang D: Artificial atlanto-odontoid joint replacement through a transoral approach. Eur Spine J 18:109-117, 2009
19. Lu B, He X, Zhao CG, Li HP, Wang D: Biomechanical study of artificial atlanto-odontoid joint. Spine 34:1893-1899, 2009
20. Ng HW, Teo EC: Nonlinear finite-element analysis of the lower cervical spine (C4–C6) under axial loading. J Spinal Disord 14: 201-210, 2001
21. Panzer MB, Cronin DS: C4–C5 segment finite element model development, validation, and load-sharing investigation. J Biomech 42:480-490, 2009
22. Puttlitz CM, Goel VK, Clark CR, Traynelis VC, Scifert JL, Grosland NM: Biomechanical rationale for the pathology of rheumatoid arthritis in the craniovertebral junction. Spine 25: 1607-1616, 2000
23. Scholes S, Unsworth A: Comparison of friction and lubrication of different hip prostheses. Proc Inst Mech Eng H 214:49-57, 2000
24. Sim HB, Lee JW, Park JT, Mindea SA, Lim J, Park J: Biomechanical evaluations of various c1-c2 posterior fixation techniques. Spine 36: E401-407, 2011
25. Tan M, Wang H, Wang Y, Zhang G, Yi P, Li Z, Wei H, Yang F: Morphometric evaluation of screw fixation in atlas via posterior arch and lateral mass. Spine 28: 888-895, 2003
26. Womack W, Leahy PD, Patel VV, Outtlitz CM: Finite element modeling of kinematic and load transmission alterations due to cervical intervertebral disc replacement. Spine 36: E1126-1133, 2011
27. Wu SK, Kuo LC, Lan HC, Tsai SW, Chen CL, Su FC: The quantitative measurements of the intervertebral angulation and translation during cervical flexion and extension. Eur Spine J 16: 1435-1444, 2007
28. Yin Q, Ai F, Zhang K, Chang Y, Xia H, Wu Z, Quan R, Mai X, Liu J: Irreducible anterior atlantoaxial dislocation: One-stage treatment with a transoral atlantoaxial reduction plate fixation and fusion. Report of 5 cases and review of the literature. Spine 30: E375-381, 2005
29. Zhang H, Bai J: Development and validation of a finite element model of the occipito-atlantoaxial complex under physiologic loads. Spine 32: 968-974, 2007